

identical with those reported previously for $\text{FeL}(\text{NO})$.⁵ Only the angular parameters differ owing to the steric constraints of the five-membered ethylenediamine chelate ring in $\text{FeL}(\text{NO})$. The Fe-N-O angle of 155.2° in $\text{FeL}'(\text{NO})$ compares favorably with the average value of 156.8° in $\text{FeL}(\text{NO})$. Thus $\text{FeL}'(\text{NO})$ provides another example⁵ of a partially bent, ordered metal nitrosyl complex at room temperature.

Both $\text{Fe}(\text{L}'\text{H})(\text{NO})_2$ and $\text{FeL}'(\text{NO})$ are paramagnetic, 17-electron species that exhibit electron spin resonance spectra. The results obtained for $\text{Fe}(\text{L}'\text{H})(\text{NO})_2$ in **1** fit in very nicely with those reported for the compounds $[\text{Fe}(\text{NO})_2\text{X}_2]^-$ where $\text{X} = \text{Cl}, \text{Br}, \text{and I}$.⁷ These dihalodinitrosyliron anions have g_{iso} values of 2.033, 2.049, and 2.072, respectively, and show no hyperfine coupling to the nitrosyl groups. The g_{iso} value measured for $\text{Fe}(\text{L}'\text{H})(\text{NO})_2$ is 2.028. In the 1:1 cocrystallized mixture of $\text{Fe}(\text{L}'\text{H})(\text{NO})_2$ and $\text{FeL}'(\text{NO})$, **2**, there was no observed magnetic interaction between the two iron centers, the closest iron-iron distance being 6.9 Å (see Figure 5). The ESR spectrum of **2** is the sum of the spectra of two species. The values for g_{iso} and A_{iso} observed for $\text{FeL}'(\text{NO})$ are the same as previously reported for this compound alone.⁵

Synthesis and Stability of $\text{Fe}(\text{L}'\text{H})(\text{NO})_2$ and Its Conversion to $\text{FeL}'(\text{NO})$ through Formal Loss of "HNO". Although small amounts of **1** and **2** were obtained in the reaction of $(\text{FeL}')_2$ with NOPF_6 , the best synthesis is the substitution reaction of $[\text{Fe}(\text{NO})_2\text{Br}_2]^-$ with $\text{L}'\text{H}_2$. In the solid state, both compounds are relatively stable and the X-ray studies were performed with the crystals exposed to the air. In solution, however, infrared spectral studies show that $\text{Fe}(\text{L}'\text{H})(\text{NO})_2$ transforms to $\text{FeL}'(\text{NO})$ upon standing for several days or during chromatography over aluminum oxide which had absorbed water. It is reasonable that, with loss of the proton, the ligand nitrogen atoms would coordinate readily to the central iron atom forming one six-membered ring and two five-membered rings.

This change in the coordination number of the iron results in reduction of the nitrosyl ligands. Formally, one of them leaves as "HNO" although the fate of the lost nitrosyl group is unknown. The remaining, coordinated nitrosyl group exhibits a decreased Fe-N-O angle, hyperfine coupling of the odd electron to the nitrosyl nitrogen nucleus, and a decrease in the NO stretching frequency in the infrared spectrum from 1740 and 1695 cm^{-1} in $\text{Fe}(\text{L}'\text{H})(\text{NO})_2$ to 1645 cm^{-1} in $\text{FeL}'(\text{NO})$. These results are reminiscent of the changes observed upon coordinating a sixth ligand to $[\text{Fe}(\text{das})_2\text{NO}]^{2+}$.¹⁸

The conversion of $\text{Fe}(\text{L}'\text{H})(\text{NO})_2$ to $\text{FeL}'(\text{NO})$ and "HNO" may be viewed as a coupled proton-electron-transfer reaction. The process is mechanistically similar to that proposed for the reduction of substrates by molybdenum enzymes¹⁹ except that the proton is donated by a ligand in the process of becoming coordinated rather than one already attached to the metal atom. The reaction of coordinated nitric oxide with acid to form HNO has been observed previously.²⁰

Acknowledgment. This work was supported by NIH Research Grant GM-16449 from the National Institute of General Medical Sciences.

Registry No. **1**, 73940-64-4; $\text{FeL}'(\text{NO})$, 64175-41-3; $[(\text{Ph}_3\text{P})_2\text{N}][\text{Fe}(\text{NO})_2\text{Br}_2]$, 61003-12-1.

Supplementary Material Available: Tables S1-S8 listing respectively final structure factor amplitudes, final atomic thermal parameters, root-mean-square amplitudes of thermal vibration, and hydrogen atom geometry for **1** and **2** (35 pages). Ordering information is given on any current masthead page.

(18) Enemark, J. H.; Feltham, R. D.; Huie, B. T.; Johnson, P. L.; Swedo, K. B. *J. Am. Chem. Soc.* **1977**, *99*, 3285 and references therein.

(19) Stiefel, E. I. *Proc. Natl. Acad. Sci. U.S.A.* **1973**, *70*, 988.

(20) Wilson, R. D.; Ibers, J. A. *Inorg. Chem.* **1979**, *18*, 336 and references cited therein.

Contribution from the Departments of Chemistry, McMaster University, Hamilton, Ontario, L8S 4M1 Canada, and Leicester University, Leicester, LE1 7RH England

Fluorine-19 and Xenon-129 NMR Studies of the $\text{XeF}_2 \cdot n\text{WOF}_4$ and $\text{XeF}_2 \cdot n\text{MoOF}_4$ ($n = 1-4$) Adducts: Examples of Nonlabile Xenon-Fluorine-Metal Bridges in Solution

JOHN H. HOLLOWAY^{1a} and GARY J. SCHROBILGEN^{*1b}

Received August 27, 1979

Xenon difluoride adducts with the weak fluoride ion acceptor species WOF_4 and MoOF_4 have been prepared and shown to possess the stoichiometries $\text{XeF}_2 \cdot \text{MOF}_4$ and $\text{XeF}_2 \cdot 2\text{MOF}_4$ ($\text{M} = \text{Mo or W}$). Fluorine-19 NMR spectroscopy has been used to study their solution structures in BrF_3 and SO_2ClF solvents. Equilibria involving higher chain length species, $\text{XeF}_2 \cdot n\text{MOF}_4$ ($n = 1-4$), have been observed at low temperatures in SO_2ClF solution. The structures have been shown to contain $\text{XeF} \cdots \text{M}$ bridges which are nonlabile on the NMR time scale at low temperatures. Isomerization between oxygen- and fluorine-bridged XeF groups, which has not previously been observed in noble-gas chemistry, has been observed in the tungsten adducts $\text{XeF}_2 \cdot n\text{WOF}_4$ ($n = 2$ and 3). The solvolytic behavior of $\text{XeF}_2 \cdot \text{MOF}_4$ adducts has also been studied, leading to the discovery of a new class of fluorosulfate-bridged species $\text{FXeO}(\text{F})\text{S}(=\text{O})\text{OMOF}_4$. Corroborating ^{129}Xe NMR data are discussed. The relative degree of covalent character in the terminal Xe-F bonds of the adduct species, as well as the relative fluoride ion acceptor strengths of MoOF_4 and WOF_4 and their polymeric chains, has been assessed on the basis of the observed ^{19}F and ^{129}Xe NMR complexation shifts. It has been concluded that WOF_4 and its polymers are stronger fluoride ion acceptors relative to XeF_2 than their MoOF_4 analogues.

Introduction

Many adducts between XeF_2 and the metal pentafluorides are known.² These have frequently been formulated as $\text{XeF}^+\text{MF}_6^-$, $\text{XeF}^+\text{M}_2\text{F}_{11}^-$, and $\text{Xe}_2\text{F}_3^+\text{MF}_6^-$ salts. From X-ray

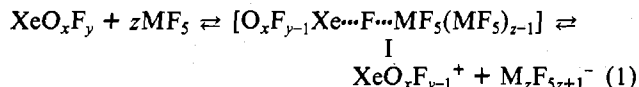
crystallographic and vibrational spectroscopic studies, it is clear, however, that a significant degree of covalent bonding between the anion and the cation must be present in the XeF^+ compounds, and, consequently, it is not entirely accurate to formulate these species as ionic compounds.³ Several prior ^{19}F NMR investigations, which have dealt with solution studies

(1) (a) Leicester University. (b) McMaster University.

(2) N. Bartlett and F. O., Sladky, "Comprehensive Inorganic Chemistry", A. F. Trotman-Dickenson, Ed., Pergamon Press, Oxford, 1973, Vol. 1, Chapter 6.

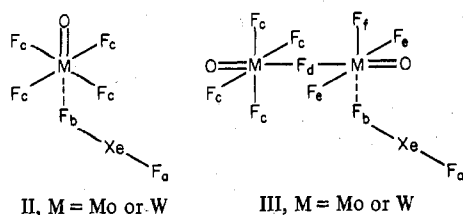
(3) R. J. Gillespie and B. Landa, *Inorg. Chem.*, **12**, 1383 (1973).

of XeF^{4+} and the higher oxidation state cations XeF_3^{+5} , XeF_5^{+6} , XeOF_3^{+5} and $\text{XeO}_2\text{F}^{+5}$ with acceptor species such as the strong Lewis acid SbF_5 , have failed to reveal evidence for anion-cation fluorine-bridge formation in solution. In these instances, the bridge interaction is presumed to be labile on the NMR time scale at the temperature at which these studies were conducted. The equilibrium (eq 1) might therefore be



expected to lie far to the right, favoring the ionic form and thus rapid fluorine redistribution by means of structure I.

Until recently, no detailed study of the relative fluoride-donor properties of xenon difluoride with fluoride acceptors in the weak to intermediate range of fluoride-acceptor strengths had been carried out either in the solid state or in solution. Indeed, it is only recently that such thermally stable adducts have been prepared when we showed that stoichiometric amounts of XeF_2 and the moderately weak fluoride acceptor WOF_4 react to form the stable solid adduct species $\text{XeF}_2 \cdot \text{WOF}_4$ and $\text{XeF}_2 \cdot 2\text{WOF}_4$.⁷ On the basis of a preliminary low-temperature ^{19}F NMR study in BrF_5 and SO_2ClF solvents and Raman spectroscopic studies of the solids, we demonstrated that the adducts are fluorine bridged to xenon and can be formulated as structures II and III. Low-temperature ^{19}F



NMR studies in these solvents revealed that fluorine exchange involving dissociation of the Xe-F bridge bond is slow, thus providing the first example of a xenon-fluorine-metal bridge which is nonlabile in solution on the NMR time scale. A single-crystal X-ray structure analysis has since shown that $\text{XeF}_2 \cdot \text{WOF}_4$ has approximately C_s symmetry.⁸ The terminal Xe-F bond length (1.89 Å) is shorter than that of XeF_2 (2.00 Å) while the Xe...F bridge-bond length (2.04 Å) is slightly longer than the Xe-F bonds in XeF_2 .

This paper presents the results of a detailed investigation of the reaction of xenon difluoride with the oxide tetrafluorides WOF_4 and MoOF_4 in solution. The study not only gives detailed information on $\text{XeF}_2 \cdot \text{WOF}_4$ and $\text{XeF}_2 \cdot 2\text{WOF}_4$ but also includes data on the hitherto unreported molybdenum analogues and provides unambiguous evidence for the existence of larger polymeric species, $\text{XeF}_2 \cdot n\text{MOF}_4$ ($n = 3$ or 4 , M = Mo and W). Moreover, studies of $\text{XeF}_2 \cdot \text{MOF}_4$ in HSO_3F solvent provide evidence for solvolysis of the adducts and for the existence of a new class of fluorosulfate-bridged species

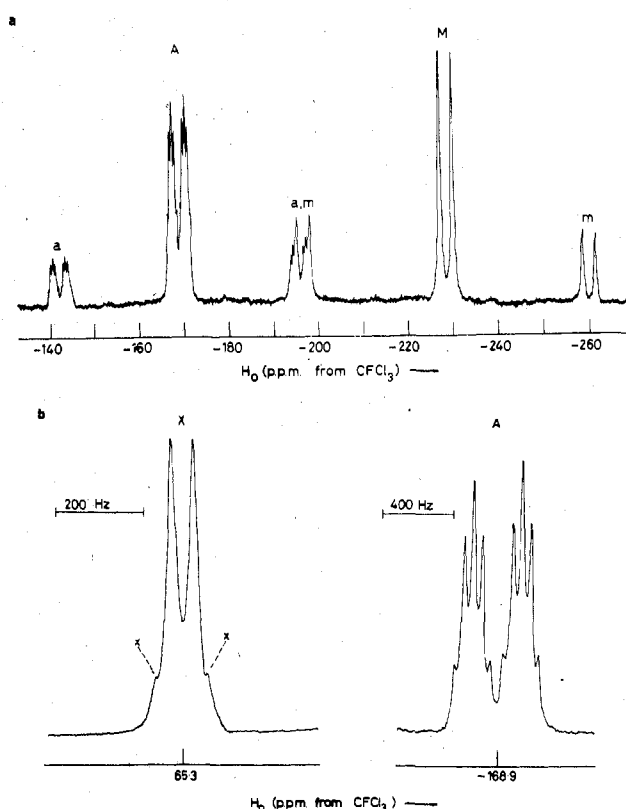
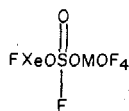


Figure 1. ^{19}F NMR spectrum (-62°C , 94.1 MHz) of $\text{XeF}_2 \cdot \text{WOF}_4$ (0.988 M, structure II) in BrF_5 solvent: (a) high-field fluorine-on-xenon region [(A) bridging fluorine, (M) terminal fluorine, and (a, m) the respective ^{129}Xe satellites]; (b) the low-field fluorine-on-tungsten environment (X) and ^{183}W satellites (x); bridging fluorine (expanded).

Recently, it has been demonstrated^{9,10} that NMR of the spin $1/2$ nuclide ^{129}Xe (natural abundance, 26.24%) can also contribute valuable corroborating structural information on xenon fluorides and their complexes, and Schrobilgen and co-workers have demonstrated that information relating to Xe-F bond ionicities can also be obtained.¹⁰ Owing to its high relative sensitivity (31.6 times that of natural abundance ^{13}C), relatively short spin-lattice relaxation times (ca. 300 μs), and the great sensitivity of ^{129}Xe chemical shifts to formal oxidation state and chemical environment, chemically bound ^{129}Xe is ideally suited for study by means of pulse-Fourier-transform NMR techniques. Pulse-Fourier-transform ^{129}Xe NMR data on the $\text{XeF}_2 \cdot n\text{MOF}_4$ ($n = 1-4$) species, which have been briefly summarized previously,¹⁰ have therefore been incorporated since they corroborate the postulated Xe-F bond ionicities and structural information.

Results and Discussion

Because of the low basicity and excellent low-temperature solvent properties of BrF_5 and SO_2ClF , the adducts of WOF_4 and MoOF_4 with XeF_2 have been studied at low temperatures in these media.

$\text{XeF}_2 \cdot \text{MOF}_4$ (M = Mo or W) in BrF_5 Solvent. The ^{19}F NMR spectra of the adducts $\text{XeF}_2 \cdot \text{WOF}_4$ and $\text{XeF}_2 \cdot \text{MoOF}_4$ are first order, belonging to the AMX_4 spin system (Figure 1 and Table I). Xenon-129 satellites arising from spin-spin coupling of ^{129}Xe with directly bonded fluorines are also ob-

(4) R. J. Gillespie, A. Netzer, and G. J. Schrobilgen, *Inorg. Chem.*, **13**, 1455 (1974).
 (5) R. J. Gillespie and G. J. Schrobilgen, *Inorg. Chem.*, **13**, 2370 (1974).
 (6) R. J. Gillespie and G. J. Schrobilgen, *Inorg. Chem.*, **13**, 765 (1974).
 (7) J. H. Holloway, G. J. Schrobilgen, and P. Taylor, *J. Chem. Soc., Chem. Commun.*, 40 (1975).
 (8) P. A. Tucker, P. A. Taylor, J. H. Holloway, and D. R. Russell, *Acta Crystallogr., Sect. B*, **31**, 906 (1975).

(9) K. Seppelt and H. H. Rupp, *Z. Anorg. Allg. Chem.*, **409**, 331, 338 (1974).
 (10) (a) G. J. Schrobilgen, J. H. Holloway, P. Granger, and C. Brevard, *Inorg. Chem.*, **17**, 980 (1978). (b) G. J. Schrobilgen, "N.M.R. and the Periodic Table", R. K. Harris and B. E. Mann, Eds., Academic Press, London, 1979, Chapter 14.

Table I. ^{19}F NMR Parameters for $\text{XeF}_2 \cdot n\text{MOF}_4$ (M = Mo or W, $n = 1-4$)

solute (molal concn)	solvent ^d	$T, ^\circ\text{C}$	species (structure)	$\delta_{19\text{F}}^b$	$J_{129\text{Xe}-19\text{F}}, \text{Hz}$	$J_{\text{F}-\text{F}}, \text{Hz}$
$\text{XeF}_2 \cdot \text{MoOF}_4$ (0.904)	BrF_5	-84	$\text{FXeF} \cdots \text{MoOF}_4$ (II)	F_a -223.1	6140 ($^{129}\text{Xe}-^{19}\text{F}_a$)	F_a-F_b 264, F_b-F_c 50
				F_b -170.0	5117 ($^{129}\text{Xe}-^{19}\text{F}_b$)	
$\text{XeF}_2 \cdot \text{WOF}_4$ (0.988)	BrF_5	-62	$\text{FXeF} \cdots \text{WOF}_4$ (II)	F_c 141.8	6150 ($^{129}\text{Xe}-^{19}\text{F}_a$)	F_a-F_b 275, F_b-F_c 50
				F_a -228.9	5016 ($^{129}\text{Xe}-^{19}\text{F}_b$)	
SO_2ClF^f -124	SO_2ClF^f	-124	$\text{FXeF} \cdots \text{MoOF}_4$ (II)	F_b -168.8	6018 ($^{129}\text{Xe}-^{19}\text{F}_a$)	F_a-F_b 267, F_a-F_c 8, F_b-F_c 47, F_a-F_b 262, F_b-F_f 46
				F_c 135.8	5110 ($^{129}\text{Xe}-^{19}\text{F}_b$)	
				F_a -219.6	5197 ($^{129}\text{Xe}-^{19}\text{F}_a$)	F_a-F_e 8, F_c-F_d 47, F_a-F_f 8, F_d-F_e 100, F_b-F_d 50,
				F_b -167.1 ^c	5110 ($^{129}\text{Xe}-^{19}\text{F}_b$)	F_d-F_f 100, F_b-F_e 46, F_e-F_f 102
				F_c 150.1		
				F_d -37.7		
				F_e 195.1		
				F_f 207.9		
				F_a -230.4	6210 ($^{129}\text{Xe}-^{19}\text{F}_a$)	F_a-F_b 266, F_c-F_g 47, F_b-F_d 50, F_b-F_e 50, F_b-F_f 50
				F_b -167 ^c	5110 ($^{129}\text{Xe}-^{19}\text{F}_b$)	
				F_c 150 ^c		
				F_d -28.9 ^c		
F_e -62.8 ^c	6200 ($^{129}\text{Xe}-^{19}\text{F}_a$)	F_a-F_b 258, F_c-F_g 48				
F_a -230.8	5000 ($^{129}\text{Xe}-^{19}\text{F}_b$)					
F_b -167 ^c						
F_c 150 ^c						
F_d -29 ^c						
F_e -64.9 ^c						
F_f -55.2						
F_a -225.7	6150 ($^{129}\text{Xe}-^{19}\text{F}_a$)	F_a-F_b 266, F_b-F_c 55				
F_b -166.8	5000 ($^{129}\text{Xe}-^{19}\text{F}_b$)					
F_c 69.7						
F_a -236.7	6260 ($^{129}\text{Xe}-^{19}\text{F}_a$)	F_a-F_b 267, F_b-F_f 60, F_b-F_d 60, F_c-F_d 60, F_b-F_c 60,				
F_b -168.4 ^c	5000 ($^{129}\text{Xe}-^{19}\text{F}_b$)	F_d-F_e 60, F_d-F_f 60				
F_c 73.2 ^c						
F_d -107.8						
F_e 119 ^d						
F_f 121 ^d						
F_a -238.7	6300 ($^{129}\text{Xe}-^{19}\text{F}_a$)	F_a-F_b 265, F_c-F_g 60				
F_b -169 ^c	5000 ($^{129}\text{Xe}-^{19}\text{F}_b$)					
F_c 73 ^c						
F_a -240.2	6315 ($^{129}\text{Xe}-^{19}\text{F}_a$)	F_c-F_d 61, F_d-F_i 64				
F_c 73 ^c						
F_d -72.0						
F_i 97.1						
F_a -243.8	6330 ($^{129}\text{Xe}-^{19}\text{F}_a$)	F_c-F_g 60, F_d-F_i 65, F_g-F_j 60, F_g-F_k 60				
F_c 73 ^c						
F_d -72 ^c						
F_g -119.3						
F_i 96.8						
SO_2ClF^f -121	SO_2ClF^f	-121	$\text{FXeF} \cdots \text{WOF}_4$ (II)	F_a -236.7	6150 ($^{129}\text{Xe}-^{19}\text{F}_a$)	F_a-F_b 266, F_b-F_c 55
				F_b -168.4 ^c	5000 ($^{129}\text{Xe}-^{19}\text{F}_b$)	
				F_c 73.2 ^c		
				F_d -107.8		
				F_e 119 ^d		
				F_f 121 ^d		
				F_a -238.7	6260 ($^{129}\text{Xe}-^{19}\text{F}_a$)	F_a-F_b 267, F_b-F_f 60, F_b-F_d 60, F_c-F_d 60, F_b-F_c 60,
				F_b -169 ^c	5000 ($^{129}\text{Xe}-^{19}\text{F}_b$)	F_d-F_e 60, F_d-F_f 60
				F_c 73 ^c		
				F_a -240.2	6315 ($^{129}\text{Xe}-^{19}\text{F}_a$)	F_c-F_d 61, F_d-F_i 64
				F_c 73 ^c		
				F_d -72.0		
F_i 97.1						
F_a -243.8	6330 ($^{129}\text{Xe}-^{19}\text{F}_a$)	F_c-F_g 60, F_d-F_i 65, F_g-F_j 60, F_g-F_k 60				
F_c 73 ^c						
F_d -72 ^c						
F_g -119.3						
F_i 96.8						

^a BrF_5 data: $\delta_{19\text{F}}(\text{F}_a) = 273.8$, $\delta_{19\text{F}}(\text{F}_e) = 136.2$, $J_{\text{F}_a-\text{F}_e} = 75$ Hz, $\delta_{19\text{F}}(\text{SO}_2\text{ClF}) = 98.5$. ^b ^{19}F chemical shifts are with respect to CFCl_3 at the sample temperature. Positive values denote chemical shifts to low field of the reference and vice versa. ^c Resonance overlaps with a resonance(s) arising from another species in the series. Alteration of the relative intensities of overlapping resonances by changing the relative concentrations of XeF_2 and MOF_4 has permitted the location of these chemical shifts. ^d Coupling constants could not be determined from this portion of the spectrum owing to poor resolution and second-order contributions. ^e Species were only observed in very low concentrations (see Table II); therefore only key NMR parameters are available. ^f See Table III for composition and relative concentrations of $\text{XeF}_2 \cdot n\text{MOF}_4$ species at equilibrium in SO_2ClF solution.

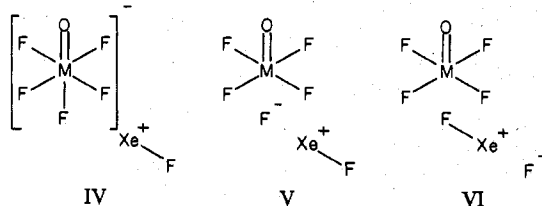
Table II. ^{129}Xe NMR Parameters for $\text{XeF}_2 \cdot n\text{MOF}_4$ ($n = 1-3$) and $\text{FXeO(F)S(=O)OMOF}_4$ ($M = \text{Mo}$ or W)^a

solute (molal concn)	$\text{XeF}_2 : \text{MOF}_4$	solvent	temp, °C	species (structure)	$\delta_{^{129}\text{Xe}}$	$J_{^{129}\text{Xe}-^{19}\text{F}}$ ^b Hz
$\text{XeF}_2 \cdot \text{WOF}_4$ (0.86)	1.00	BrF_5	-66	$\text{FXeF} \cdots \text{WOF}_4$ (II)	-1331	{5051 b 6196 a
$\text{XeF}_2 \cdot \text{MoOF}_4$ (0.92)	1.00	BrF_5	-80	$\text{FXeF} \cdots \text{MoOF}_4$ (II)	-1381	{5117 b 6139 a
$\text{XeF}_2 \cdot 2\text{WOF}_4$ (0.70)	2.00	SO_2ClF	-115	$\text{FXeF} \cdots \text{WOF}_4$ (II)	-1315	{5000 b 6127 a
				$\text{FXeF} \cdots \text{WOF}_4(\text{WOF}_4)$ (III)	-1189	{4964 b 6268 a
				$\text{FXeF} \cdots \text{WOF}_4(\text{WOF}_4)_2$ (VII)	-1170	{4996 b 6304 a
				$\text{FXeOWF}_2(\text{WOF}_4)$ (IX)	-955	6373
				$\text{FXeOWF}_2(\text{WOF}_4)_2$ (X)	-906	6373
XeF_2 (0.98) MoOF_4 (2.13)	2.17	SO_2ClF	-118	$\text{FXeF} \cdots \text{MoOF}_4(\text{MoOF}_4)$ (III)	-1338	{5036 b 6159 a
				$\text{FXeF} \cdots \text{MoOF}_4(\text{MoOF}_4)_2$ (VII)	-1321	{5029 b 6156 a
$\text{XeF}_2 \cdot \text{MoOF}_4$ (1.32)	1.00	HSO_3F	-100	{ FXeOSO_2F $\text{FXeO(F)S(=O)OMoOF}_4$	{-1407 -1342	{6051 5971
$\text{XeF}_2 \cdot \text{WOF}_4$ (1.00)	1.00	HSO_3F	-90	{ FXeOSO_2F $\text{FXeO(F)S(=O)OWOF}_4$	{-1416 -1335	{6021 6131
XeF_2 ^c (2.70)		BrF_5	-40	XeF_2	-1708	5583
XeF_2 ^c (0.71)		SbF_5	25	XeF^+	-574	7207
$\text{Xe}_2\text{F}_3^+ \text{AsF}_6^-$ ^c (1.14)		BrF_5		$(\text{FXe})_2\text{F}^+$	-1051	{4865 b 6740 a

^a Spectra were recorded at 22.63 MHz in the FT mode and were referenced with respect to external neat liquid XeOF_4 at 25 °C. ^b All $^{129}\text{Xe}-^{19}\text{F}$ spin-spin couplings appear as doublets. For fluorine-bridged species, b and a denote coupling of ^{129}Xe with the bridging and terminal fluorines on xenon, respectively. ^c Reference 9.

served for the A and M environments in the ^{19}F NMR spectra. The spectra are, therefore, consistent with the nonlabile fluorine-bridged structure II in which there is free rotation about the $\text{M} \cdots \text{F}$ bond in solution.

The chemical shift of terminal fluorine on xenon occurs at significantly lower frequency than that of the bridging fluorine. A parallel trend has been noted for the fluorine-bridged cation Xe_2F_3^+ in BrF_5 solvent⁴ (Table I). The observed relative chemical shifts may be rationalized in terms of valence bond structures IV-VI. The contribution from structure IV is



presumed to give rise to a net high-frequency shift in the ^{19}F resonance of the bridging fluorine (cf. chemical shifts of the axial fluorines of WOF_5^- , -81 ppm, and MoOF_5^- , -47 ppm, in propylene carbonate solvent¹¹) relative to the contributions from structures V and VI which, effectively, represent the valence bond description of XeF_2 (cf. XeF_2 , Table I). Structure IV also gives rise to a low-frequency ^{19}F chemical shift relative to that of XeF_2 which is presumed to arise from increased $\text{Xe}-\text{F}^+$ character of the terminal $\text{Xe}-\text{F}$ bond (cf. XeF^+ , Table I). It has been previously shown that the covalent character of the $\text{Xe}-\text{F}$ bond in xenon(II) species can be correlated with the ^{19}F chemical shift and $^{129}\text{Xe}-^{19}\text{F}$ coupling constant.^{4,6} In general, both parameters also correlate with the observed bridging and terminal $\text{Xe}-\text{F}$ bond lengths where these are known.⁴ Analogous trends are observed for the 1:1 adducts of XeF_2 with MOF_4 .

The fluorine-fluorine spin-spin couplings for the terminal and bridge fluorines directly bonded to xenon in $\text{XeF}_2 \cdot \text{MOF}_4$

(Table I) are similar in magnitude to those observed for Xe_2F_3^+ (308 Hz)⁴ and Kr_2F_3^+ (349 Hz).¹² In other fluoro and oxyfluoro cations of xenon which have been studied, the fluorine-fluorine coupling constant is comparatively small (103-176 Hz). The large difference between the values has been associated with the size of the $\text{F}-\text{Ng} \cdots \text{F}$ ($\text{Ng} = \text{Kr}$ or Xe) angle, which is $\sim 180^\circ$ in Xe_2F_3^+ and Kr_2F_3^+ (and $\text{XeF}_2 \cdot \text{MOF}_4$) but is only $\sim 90^\circ$ in the other cations.^{4,12} Fluorine-fluorine spin-spin coupling is also observed between the four equivalent fluorines on the metal and the bridging fluorine, which gives rise to 1:4:6:4:1 quintet fine structure on each of the doublet branches of the bridging fluorine and doublet fine structure on the fluorine-on-metal resonance in the tungsten adduct. The magnitude of the coupling is very similar to that observed for the spin-spin coupling constant between the axial and equatorial fluorines in the WOF_5^- (53 Hz)¹¹ and MoOF_5^- (50 Hz)¹¹ anions and between the bridging fluorine and equatorial fluorines of the $\text{W}_2\text{O}_2\text{F}_9^-$ (58 Hz)¹¹ and $\text{Mo}_2\text{O}_2\text{F}_9^-$ (55 Hz)¹¹ anions. Although this coupling was not resolved for the molybdenum adduct in BrF_5 , it was resolved in SO_2ClF at lower temperatures where the residual fluorine exchange was slowed (see subsequent discussion).

Fluorine-on-metal environments, F_c , which occur at significantly higher frequencies than fluorine-on-xenon environments, appear as simple first-order doublets in the ^{19}F NMR spectra (Figure 1b). There is no evidence for long-range spin-spin coupling between ^{129}Xe and the fluorines on the metal in either the tungsten or molybdenum complexes. Spin-spin coupling between the four equivalent fluorines on tungsten and ^{183}W ($I = 1/2$, 14.28%) is observed in $\text{XeF}_2 \cdot \text{WOF}_4$ (Table I and Figure 1b) and is similar to those previously reported for equatorial fluorines on tungsten in WOF_5^- (70 Hz)¹¹ and $\text{W}_2\text{O}_2\text{F}_9^-$ (70 Hz).¹¹ Similar couplings with the nuclides ^{95}Mo ($I = 5/2$, 15.78%) and ^{96}Mo ($I = 5/2$, 9.80%) are not observed for $\text{XeF}_2 \cdot \text{MoOF}_4$ in either BrF_5 or SO_2ClF , presumably because of quadrupole relaxation.

(11) R. Bougon, T. Bui Huy, and P. Charpin, *Inorg. Chem.*, **14**, 1822 (1975).(12) R. J. Gillespie and G. J. Schrobilgen, *Inorg. Chem.*, **15**, 22 (1976).

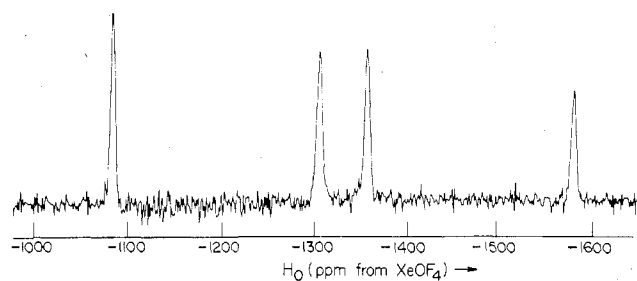
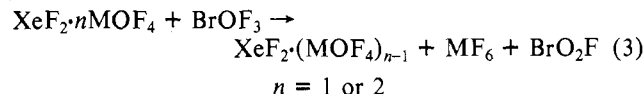
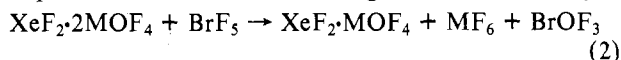


Figure 2. ^{129}Xe NMR spectrum (-66°C , 22.6 MHz) of $\text{XeF}_2\cdot\text{WOF}_4$ (0.86 *m*, structure II) in BrF_5 solvent.

The ^{129}Xe NMR spectra of both the molybdenum and tungsten species belong to the AMX spin system. The observed doublet of doublets fine structure in the ^{129}Xe spectra of both species (Figure 2) is consistent with an F–Xe–F group in which one fluorine is bonded to the MOF_4 group. The high-frequency shifts of the ^{129}Xe resonances relative to that of XeF_2 is also consistent with enhancement of XeF^+ character in the complexes (cf. XeF_2 and XeF^+ , Table II). The ^{129}Xe chemical shifts of $\text{XeF}_2\cdot\text{MOF}_4$ are, however, substantially less than that of Xe_2F_3^+ (Table II). It is interesting to note that, despite the larger measure of XeF^+ character in Xe_2F_3^+ , it is also nonlabile in BrF_5 solution at comparable temperatures and concentrations.

The relative fluoride-acceptor strengths of WOF_4 and MoOF_4 are readily deduced from ^{129}Xe and ^{19}F chemical shift data. The high-frequency complexation shift of the ^{129}Xe resonance of $\text{XeF}_2\cdot\text{WOF}_4$ clearly shows enhancement of XeF^+ character relative to that of $\text{XeF}_2\cdot\text{MoOF}_4$. The opposite trend is exhibited by the ^{19}F NMR resonance of the terminal fluorine on xenon which increases with increasing XeF^+ character while that of the bridge ^{19}F resonance decreases. Thus, it may be concluded that WOF_4 is a stronger fluoride acceptor toward XeF_2 and, presumably, other fluoride ion donors than MoOF_4 .

$\text{XeF}_2\cdot n\text{MOF}_4$ ($n \geq 2$, $M = \text{Mo}$ or W) in SO_2ClF Solvent. Dissolution of $\text{XeF}_2\cdot 2\text{WOF}_4$ and $\text{XeF}_2\cdot 2\text{MoOF}_4$ as well as mixtures of the 1:2 adduct and excess oxide tetrafluoride in BrF_5 led to rapid decomposition to the corresponding metal hexafluorides and presumably BrOF_3 and BrO_2F , according to eq 2 and 3. Eventual darkening of the solution to yellow



low-brown is attributed to further decomposition of BrOF_3 and BrO_2F to BrF_3 , Br_2 , and O_2 .¹³ Unlike the 1:1 adducts, the 1:2 adducts apparently undergo partial dissociation in BrF_5 solvent giving free MOF_4 , which is rapidly fluorinated by the solvent. Both the 1:1 and 1:2 adducts as well as their mixtures with excess of oxide tetrafluoride are very soluble at low temperatures in SO_2ClF . By addition of excess MOF_4 to solutions of the pure compounds, it was possible to vary the ratio $\text{XeF}_2\cdot\text{MOF}_4$ over the ranges 1.48–2.35 and 1.37–3.04 for the tungsten and molybdenum systems, respectively.

NMR Spectra of ^{19}F on Xe and of ^{129}Xe . The low-temperature ^{19}F NMR spectra of these solutions are more complex than would be expected for simple mixtures of excess MOF_4 with the 1:1 (structure II) and 1:2 (structure III) fluorine-bridged species. The F-on-Xe regions of the ^{19}F NMR spectra are well resolved and clearly indicate that several xenon species are present in equilibrium (Figure 3). The series of lowest frequency doublets with accompanying ^{129}Xe satellites observed

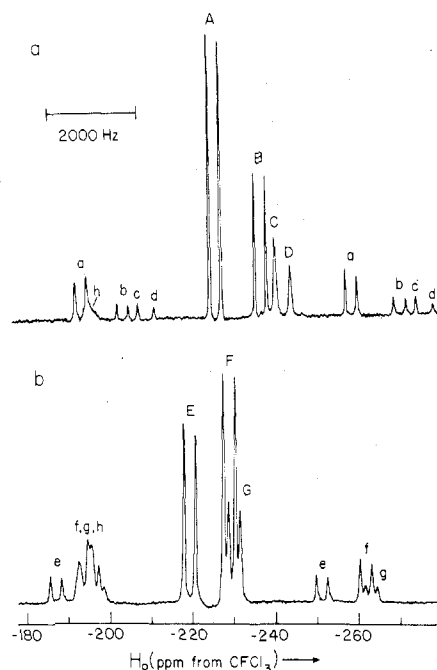


Figure 3. ^{19}F NMR spectra (94.1 MHz, SO_2ClF solvent) depicting the terminal fluorine-on-xenon region for equilibrated mixtures of (a) $\text{XeF}_2\cdot\text{WOF}_4$ (0.433 *m*) and $\text{XeF}_2\cdot 2\text{WOF}_4$ (0.393 *m*) recorded at -121°C [(A) structure II, (B) structure III, (C) structure IX, (D) structure X]; (b) XeF_2 (1.096 *m*) and MoOF_4 (2.169 *m*) recorded at -124°C [(E) structure II, (F) structure III, (G) structure VII]. a–g designate the respective ^{129}Xe satellites and h represents overlapping ^{129}Xe satellites arising from the bridging fluorines.

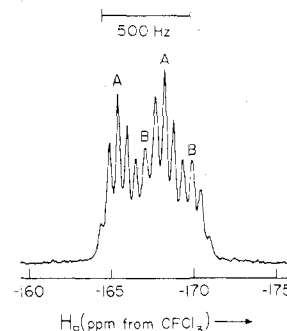
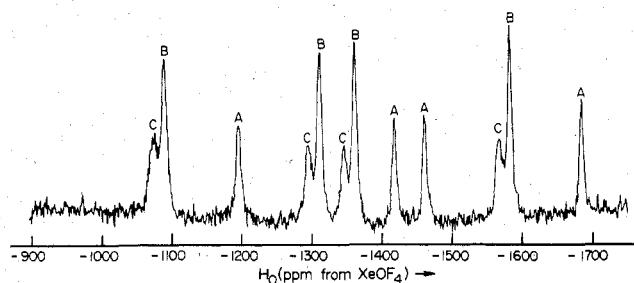


Figure 4. ^{19}F NMR spectrum (-121°C , 94.1 MHz) of the bridging fluorine-on-xenon region for an equilibrated mixture of $\text{XeF}_2\cdot 2\text{WOF}_4$ (0.393 *m*) and $\text{XeF}_2\cdot\text{WOF}_4$ (0.433 *m*) in SO_2ClF solvent. A and B designate the centers of the binomial quintets arising from the bridging fluorines of structures II and III, respectively.

in both the molybdenum and tungsten systems clearly arise from several fluorine-bridged terminal Xe–F groups which are spin–spin coupled to the bridging fluorine. The corresponding series of overlapping bridging environments occur at high frequencies and show spin–spin coupling to the terminal fluorine-on-xenon and adjacent fluorine-on-metal environment(s) as well as ^{129}Xe satellites. The fine structure on the bridging fluorines consists of a doublet of quintets (or pseudoquintets), indicating that coupling between the bridging fluorine-on-xenon and the fluorines on the adjacent metal are all nearly equal (Figure 4). Under high-resolution conditions, quintet or pseudoquintet fine structure arising from long-range spin–spin coupling with the adjacent fluorine-on-metal environment(s) was also observed on the doublet of the terminal fluorine-on-xenon for $\text{XeF}_2\cdot\text{MoOF}_4$ (8 Hz) and $\text{XeF}_2\cdot 2\text{MoOF}_4$ (8 Hz). A series of singlets with accompanying ^{129}Xe satellites was also observed in the ^{19}F NMR spectra of the tungsten systems which have no counterpart in the molybdenum systems

Table III. Relative Integrated ^{19}F NMR Intensities of the Terminal XeF Groups for Equilibrium Mixtures of $\text{XeF}_2 \cdot n\text{MOF}_4$ ($M = \text{Mo}$ or W) in SO_2ClF Solvent at -121°C

M	[MOF ₄]/[XeF ₂]	initial molal concn of XeF ₂	rel ^{19}F NMR intensities of terminal Xe-F groups					
			II	III	VII	VIII	IX	X
Mo	1.37	0.95	1.97	1.00	0.14			
	1.98	1.10	0.66	1.00	0.46			
	3.04	0.79	0.40	1.00	1.01	0.20		
W	1.48	0.83	2.21	1.60	0.06			1.00
	2.00	0.88	1.39	1.67	0.18			1.00
	2.35	0.66	0.46	1.60	0.39			1.00

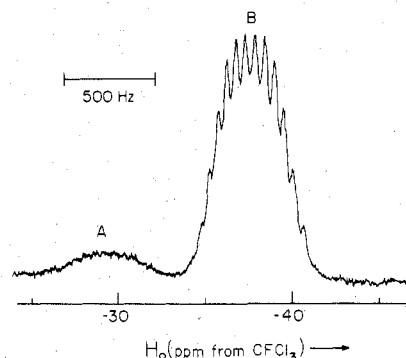
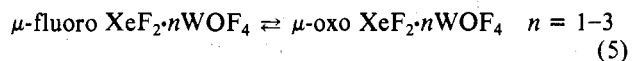
Figure 5. ^{129}Xe NMR spectrum (-118°C , 22.6 MHz) of an equilibrated mixture of XeF_2 (0.98 *m*) and MoOF_4 (2.13 *m*) in SO_2ClF solvent [(A) structure II, (B) structure III, (C) structure VII].

(Figure 3a). These singlets are assigned to oxygen-bridged terminal Xe-F groups. The ^{129}Xe NMR results (Table II) clearly confirm the ^{19}F NMR assignments. The presence of several overlapping doublets of doublets confirms the existence of an equal number of fluorine-bridged terminal Xe-F groups while the added presence of simple doublets confirms the existence of oxygen-bridged terminal Xe-F groups in the tungsten system.

By altering the initial relative amounts of XeF_2 and MOF_4 present in SO_2ClF solution and observing the effects on relative intensities of the ^{129}Xe spectra and fluorine-on-xenon environments in the ^{19}F NMR spectra at equilibrium at low temperature (Tables I and III), it was possible to assign the terminal fluorine-on-xenon resonances to their respective mononuclear and polynuclear tungsten and molybdenum species. Species assignable to μ -fluoro $\text{XeF}_2 \cdot n\text{MOF}_4$ ($M = \text{W}$ or Mo , $n = 1-3$, structures II, III, and VII), μ -fluoro $\text{XeF}_2 \cdot 4\text{MoOF}_4$ (structure VIII), and μ -oxo $\text{XeF}_2 \cdot n\text{WOF}_4$ ($n = 2$ or 3 , structures IX and X) were identified (Tables I and II). The assignments are consistent with the anticipated relative order of basicities of the corresponding mono- and polynuclear anions, giving rise to more XeF^+ character (decreasing frequency) for the terminal XeF group with decreasing basicity (increasing chain length) in the ^{19}F NMR spectra. This trend is confirmed by the ^{129}Xe NMR results (Table II and Figure 5), which show an increase in frequency (increasing XeF^+ character) with increasing chain length. In general, decreasing basicity of the polynuclear chain is noted to attenuate rapidly with increasing chain length in both the μ -fluoro and μ -oxo species.

Xe-F \leftrightarrow Xe-O Bond Isomerization in Tungsten Systems. Isomerization between fluorine-bridged and oxygen-bridged Xe-F groups is unprecedented in noble-gas chemistry. A study of the ^{19}F NMR intensities of the terminal Xe-F environment at -121°C in the tungsten system shows that relative intensities for the dinuclear and trinuclear species are independent of initial relative concentrations of XeF_2 and WOF_4 , confirming the assignment of these resonances to isomeric pairs of μ -oxo and μ -fluoro species (Table III). The equilibrium constants (eq 4) corresponding to eq 5 also show that fluo-

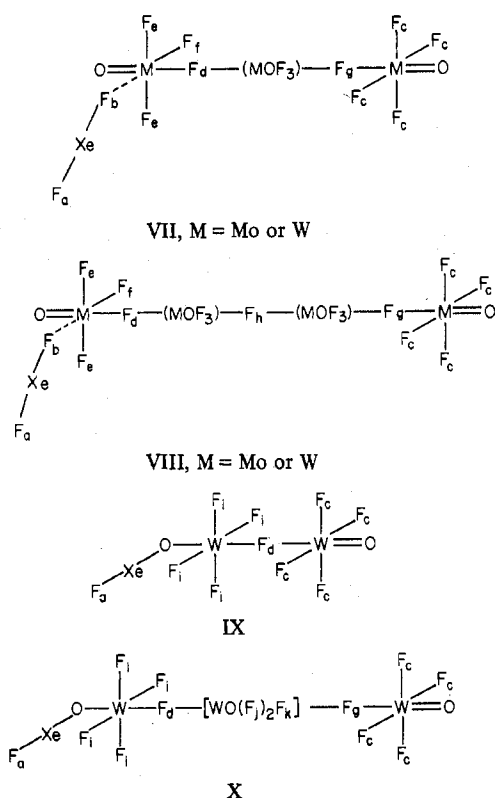
$$K_n = [\mu\text{-oxo } \text{XeF}_2 \cdot n\text{WOF}_4] / [\mu\text{-fluoro } \text{XeF}_2 \cdot n\text{WOF}_4] \quad (4)$$

Figure 6. ^{19}F NMR spectrum (-124°C , 94.1 MHz) depicting the Mo-F-Mo bridge environments, F_d , for an equilibrated mixture of XeF_2 (0.954 *m*) and MoOF_4 (1.305 *m*) in SO_2ClF solvent [(A) structure VIII, (B) structure III].

rine-bridge formation is more highly favored in the case of the shorter tungsten chain species. The respective equilibrium constants have been calculated from the ^{19}F NMR intensities of the terminal Xe-F groups at -121°C : $K_1 = \sim 0$, $K_2 = 0.62 \pm 0.02$, $K_3 = 8.8 \pm 1.2$.

An empirical plot of $\delta_{^{19}\text{F}}$ for the terminal fluorine-on-xenon vs. $\delta_{^{129}\text{Xe}}$ for xenon(II) structures, in which the XeF group is bonded to either oxygen or fluorine, yields separate near-linear correlations for each type of XeF group.⁹ The relative degree of ionic character in the Xe-O bond or Xe...F bridge bond can be empirically assessed by using these correlations. It may be inferred that the μ -oxo species possesses more XeF^+ character than any oxygen-bonded XeF group observed so far. In fact, the degree of ionicity is very similar to that of XeF^+ in HSO_3F solution ($\delta_{^{129}\text{Xe}} = -911$ at -70°C and $\delta_{^{19}\text{F}} = -243$ at -96°C). The ionic nature of the Xe-O bond and failure to observe any evidence for the existence of analogous oxygen-bonded molybdenum structures is consistent with the $\text{W}_2\text{O}_2\text{F}_9^-$ and $\text{W}_3\text{O}_3\text{F}_{13}^-$ anions' greater abilities to accommodate negative charge than their molybdenum counterparts.

NMR Spectra of ^{19}F on M. The existence of polymeric chains comprising of up to four MOF_4 molecules linked together by M-F-M bridges is further confirmed by the observation of bridging fluorine resonances in the ^{19}F NMR spectra of equilibrated mixtures of the adducts. These environments are less shielded than their counterparts in $\text{W}_2\text{O}_2\text{F}_9^-$ and $\text{Mo}_2\text{O}_2\text{F}_9^-$ (-146 and -135 ppm, respectively, in propylene carbonate solution¹¹) and occur in the -30 to -120 ppm region of the spectrum. The Mo-F-Mo bridge environments of the 1:2 and 1:3 μ -fluoro complexes, structures III and VII, respectively, are for the most part well separated. Fine structure has been resolved on F_d (-37.7 ppm) of the 1:2 molybdenum species, giving a 12-line nonbinomial multiplet (Figure 6) whose coupling constants have been estimated (Table I) by assuming the geometry represented by structure III. Two broad, unresolved lines of equal intensity corresponding to the two Mo-F-Mo bridge environments F_d and F_g of μ -fluoro $\text{XeF}_2 \cdot 3\text{MoOF}_4$ (structure VII) have also been observed (-28.9 and -62.8 ppm) in equilibrated mixtures at -121°C . At high relative proportions of MoOF_4 , an additional species was ob-



served in low concentration which has been assigned to $\text{XeF}_2 \cdot \text{MoOF}_4$ (structure VIII). Only two of the three expected Mo-F-Mo bridge environments associated with this structure have been observed. These occur at -64.9 (F_g) and -55.2 (F_h) ppm and are broad and lacking in fine structure. The third environment is presumed to be coincident with F_d in the 1:3 adduct, i.e., ca. -29 ppm.

It is clear from the relative integrated intensities that the ^{19}F resonances corresponding to the W-F-W fluorine bridges trans to the Xe-O bonds in μ -oxo $\text{XeF}_2 \cdot n\text{WOF}_4$ ($n = 2$ or 3 , structure IX and X) are coincident. A symmetric pseudononet (-72.0 ppm) is, however, observed for these environments at low $\text{WOF}_4:\text{XeF}_2$ ratios (low concentrations of μ -oxo $\text{XeF}_2 \cdot 3\text{WOF}_4$) having a splitting of 61 Hz. The fine structure is assigned to F_d in μ -oxo $\text{XeF}_2 \cdot 2\text{WOF}_4$ (structure IX). At high proportions of $\text{WOF}_4:\text{XeF}_2$, i.e., 2.35:1.00, the multiplet fine structure cannot be resolved owing, presumably, to overlap with F_d in structure X. A broad low-frequency "nonet" (60-Hz splittings) was also observed at -119.3 ppm and is assigned to the more highly shielded fluorine of the W-F-W bridge, F_d , located trans to the terminal W=O bond in μ -oxo $\text{XeF}_2 \cdot 2\text{WOF}_4$ (structure X). Finally, a "nonet" (60-Hz splittings) observed at -107.8 ppm is assigned to the bridge environment F_d arising from μ -fluoro $\text{XeF}_2 \cdot 2\text{WOF}_4$ (structure III). The observed pseudo-binomial nonet structures on F_d of structures IX and III and on F_g of structure X indicates that the eight fluorine environments cis to these bridging fluorines possess essentially the same values for their respective coupling constants. In structure X, both fluorine-bridge resonances F_g and F_d (coincident with F_d of structure IX) were shown to increase simultaneously when the relative amount of WOF_4 was increased, thus confirming their assignments. No separate fluorine-bridge resonances attributable to μ -fluoro $\text{XeF}_2 \cdot 3\text{WOF}_4$ could be observed and are presumed either to be too weak and broad (Table III) or to overlap with the more intense fluorine-bridge resonances of μ -fluoro $\text{XeF}_2 \cdot 2\text{WOF}_4$, μ -oxo $\text{XeF}_2 \cdot 2\text{WOF}_4$, and μ -oxo $\text{XeF}_2 \cdot 3\text{WOF}_4$.

The doublet fine structures associated with the four equivalent fluorines, F_c , of the terminal MOF_4 groups in structures II and III and VII-X have also been assigned for

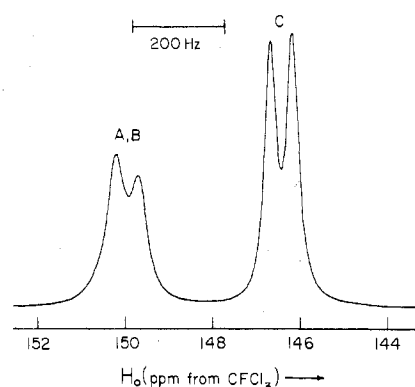


Figure 7. ^{19}F NMR spectrum (-124°C , 94.1 MHz) depicting the terminal MOF_4 environments, F_c , for an equilibrated mixture of XeF_2 (0.954 *m*) and MoOF_4 (1.305 *m*) in SO_2ClF solvent [(A) structure VII, (B) structure III, (C) structure II].

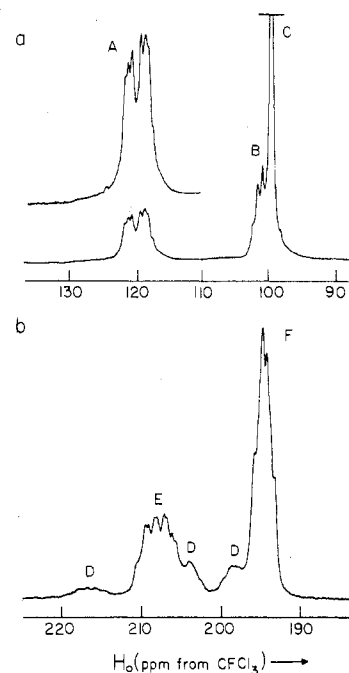


Figure 8. ^{19}F NMR spectra (94.1 MHz, SO_2ClF solvent) depicting the nonbridging and nonterminal fluorine-on-tungsten and -molybdenum regions for equilibrated mixtures: (a) $\text{XeF}_2 \cdot \text{WOF}_4$ (0.433 *m*) and $\text{XeF}_2 \cdot 2\text{WOF}_4$ (0.393 *m*) at -121°C [A and B designate F_f and F_c , respectively, of structure III, and C designates SO_2ClF solvent]; (b) XeF_2 (0.954 *m*) and MoOF_4 (1.305 *m*) at -124°C . D is unassigned; E and F designate F_f and F_c , respectively, of structure III.

equilibrated $\text{XeF}_2/\text{MOF}_4$ mixtures in SO_2ClF and indicate that all of the adduct chains terminate in an MOF_4 group having their oxygen trans to the M-F-M fluorine bridge (Figure 7). In structure III, this resonance occurs at lower frequency than in the polymeric cases. Unfortunately, the ^{19}F resonances of the terminal MOF_4 group corresponding to polymeric structures are all nearly coincident as is evidenced by increased skewing and concomitant loss of resolution on the doublet with increasing relative proportions of MOF_4 (Figure 7).

At low $\text{MoOF}_4:\text{XeF}_2$ ratios it has been possible to assign resonances arising from F_e and F_f in $\text{XeF}_2 \cdot 2\text{MOF}_4$ (structure III). At low $\text{MOF}_4:\text{XeF}_2$ ratios both $\text{XeF}_2 \cdot \text{MOF}_4$ and $\text{XeF}_2 \cdot 2\text{MOF}_4$ dominate (Figure 8). For example, the fluorine-on-molybdenum resonances arising from F_e in the 1:1 (147.7 ppm) and 1:2 (150.1 ppm) adducts are well separated while F_c (196.1 ppm) and F_f (207.9 ppm) of $\text{XeF}_2 \cdot 2\text{MoOF}_4$ occur at higher frequency and are readily assigned on the basis

Table IV. ^{19}F NMR Parameters for $\text{FXeO}(\text{F})\text{S}(=\text{O})\text{OMOF}_4$ and Related Systems in HSO_3F^a

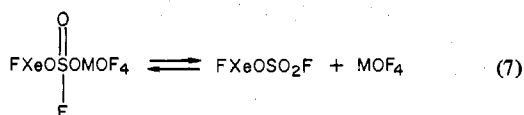
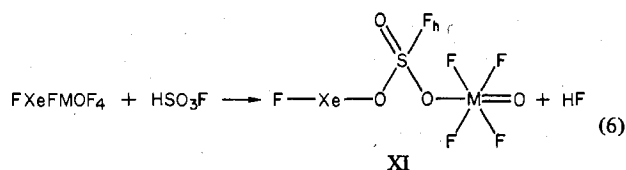
solute (molal concn)	temp, °C	$\text{FXeO}(\text{F})\text{S}(=\text{O})\text{OMOF}_4$				FXeOSO_2F				δ^a				
		δ^a				δ^a				Xe- (SO_3^- - $\text{F})_2$	HSO ₃ - F	S ₂ - O ₆ F ₂	MOF ₄	HF
		F on Xe	F on S	F on M	$J_{129}\text{Xe}-^{19}\text{F}$, Hz	F on Xe	F on S	$J_{129}\text{Xe}-^{19}\text{F}$, Hz						
$\text{XeF}_2 \cdot \text{WOF}_4$ (1.52)	-90	-204.3	<i>b</i>	67.8	5992	-196.9	40.2	5942	43.0	40.8	39.0	69.2	-180.7	
$\text{XeF}_2 \cdot \text{MoOF}_4$ (2.32)	-97	-201.6	<i>b</i>	146.8	5853	-194.5	40.1	5924	42.7	40.7	38.8	<i>c</i>	-183.2	
WOF_4 (2.19)	-84									40.8		69.1		
MoOF_4 (0.45)	-80									40.9		148.6		

^a Spectra were recorded at 94.1 MHz in the CW mode and were referenced with respect to external CFCl_3 at the sample temperature.

^b Not observed and presumed to be nearly coincident with the HSO_3F solvent line. ^c Not observed and presumed to be exchanging with $\text{FXeO}(\text{F})\text{S}(=\text{O})\text{OMoOF}_4$.

of their integrated relative intensities (Figure 8b). A small proportion (~4 mol %) of $\text{XeF}_2 \cdot 3\text{MoOF}_4$ is also present at this ratio and exhibits weak, broad resonances which partially overlap with F_c and F_f of $\text{XeF}_2 \cdot 2\text{MoOF}_4$. As indicated earlier in this discussion, F_c of $\text{XeF}_2 \cdot 3\text{MoOF}_4$ is coincident with the corresponding $\text{XeF}_2 \cdot 2\text{MoOF}_4$ environment. Analogous assignments have been made for μ -fluoro $\text{XeF}_2 \cdot 2\text{WOF}_4$ (Figure 8a). The remaining fluorine-on-metal environments of the polynuclear chains, which are generally broad and lacking in fine structure, overlap severely with one another in the equilibrated mixtures. With the exception of μ -fluoro $\text{XeF}_2 \cdot 2\text{MoOF}_4$, no attempts have, therefore, been made to assign these regions of the spectra in detail. Consequently it has not been possible to determine whether the fluorine bridges are cis or trans with respect to the oxygen in the nonterminal MOF_4 groups of structures VII, VIII, and X.

$\text{XeF}_2 \cdot \text{MOF}_4$ in HSO_3F Solvent. Xenon difluoride complexes containing weak $\text{Xe} \cdots \text{F}$ bridge bonds such as $\text{XeF}_2 \cdot \text{MF}_5$ ($M = \text{As}$ or Sb) and $\text{XeF}_2 \cdot 2\text{SbF}_5$ do not undergo solvolysis in HSO_3F at low temperatures. The strongly fluorine-bridged cation $(\text{FXe})_2\text{F}^+$, however, forms the fluorosulfate-bridged cation $(\text{FXe})_2\text{SO}_3\text{F}^+$ and HF .¹⁴ Likewise, the fluorine-bridged oxide tetrafluoride adducts $\text{XeF}_2 \cdot \text{MoOF}_4$ and $\text{XeF}_2 \cdot \text{WOF}_4$ possess rather strong $\text{Xe}-\text{F}$ bridge bonds and undergo analogous solvolysis reactions at -80°C according to eq 6 to give a new species with a fluorosulfate-bridged structure (XI) in equilibrium with FXeSO_3F and MOF_4 (eq 7).



The proposed reactions and equilibria are confirmed by ^{19}F (Table IV) and ^{129}Xe (Table II) NMR spectroscopy. In addition to a solvent line at 40.8 ppm and an HF line at -182.0 ppm, two new ^{19}F resonances were observed which can be assigned to the fluorosulfate-bridged structure XI. The singlets at 67.8 and 146.8 ppm are assigned to the four equivalent fluorines on the metal, and the low-frequency singlets at -204.3 and -201.6 ppm, which possess ^{129}Xe satellites, are assigned to the terminal fluorine on xenon in the tungsten and molybdenum species, respectively. The terminal nature of the fluorine on xenon in structure XI was confirmed by the ^{129}Xe spectra which consisted of a doublet due to $^{129}\text{Xe}-^{19}\text{F}$ spin-spin coupling centered at -1335 and -1342 ppm for the respective

tungsten and molybdenum species. Additional sets of ^{19}F and ^{129}Xe lines arising from equilibrium 7 were observed in both systems. Two ^{19}F singlets at 40.2 and -195.7 ppm have been assigned to fluorine on sulfur and fluorine on xenon, respectively, in FXeSO_3F . The low-frequency FXeSO_3F singlet also displayed ^{129}Xe satellites ($J_{129}\text{Xe}-^{19}\text{F} = 6036$ Hz). A separate MOF_4 peak was not observed for free MoOF_4 but was observed for free WOF_4 . Molybdenum oxide tetrafluoride, being a weaker Lewis acid than WOF_4 , presumably undergoes rapid exchange with structure XI in solution, giving a single exchange-averaged line for fluorine on molybdenum. Fluorine-on-sulfur signals arising from structure XI could not be observed in either molybdenum or tungsten samples and were presumed to be coincident with the HSO_3F solvent line. The ^{129}Xe spectra of both species in HSO_3F also showed an additional doublet assignable to FXeSO_3F (-1412 ppm, $J_{129}\text{Xe}-^{19}\text{F} = 5996$ Hz).

Experimental Section

Materials. Xenon difluoride¹⁵ and SO_2ClF ¹⁶ were prepared as described elsewhere. Tungsten oxide tetrafluoride was prepared in a quartz system by passing a mixture of F_2 and O_2 (~5:1) over tungsten powder (99.9%, BDH Chemicals, Ltd.) in a nickel boat heated to $\sim 400^\circ\text{C}$. The resulting WOF_4 collected on the cooler surfaces of the reaction vessel while WF_6 , also produced in the reaction, was trapped out at -196°C . Molybdenum oxide tetrafluoride was prepared by heating molybdenum powder (99.9%, BDH Chemicals, Ltd.) and a stoichiometric amount of O_2 and F_2 (20% excess) in a closed nickel vessel at 350°C for 8 h. The resulting product was sublimed out of the reaction vessel through a high-temperature valve at 170°C and was collected in a Pyrex vessel at -78°C . Both WOF_4 and MoOF_4 were resublimed in Pyrex vessels and stored in Kel-F containers in a drybox.

The adducts $\text{XeF}_2 \cdot \text{MOF}_4$ and $\text{XeF}_2 \cdot 2\text{MOF}_4$ ($M = \text{Mo}$ or W) were prepared by fusing stoichiometric amounts of XeF_2 and MOF_4 together at $50-60^\circ\text{C}$ in 7-mm o.d. FEP tubes equipped with Teflon valves to give clear colorless liquids which crystallized at room temperature. In typical preparations, the following amounts of reactants were used: $\text{XeF}_2 \cdot \text{WOF}_4$, 4.284 mmol of XeF_2 and 4.252 mmol of WOF_4 ; $\text{XeF}_2 \cdot 2\text{WOF}_4$, 3.904 mmol of XeF_2 and 7.766 mmol of WOF_4 ; $\text{XeF}_2 \cdot \text{MoOF}_4$, 6.459 mmol of XeF_2 and 6.315 mmol of MoOF_4 ; $\text{XeF}_2 \cdot 2\text{MoOF}_4$, 5.675 mmol of XeF_2 and 11.354 mmol of MoOF_4 . Adduct purities were confirmed by recording their Raman spectra at -100 to -110°C . The vibrational spectra are discussed in detail elsewhere.¹⁷ Purification of solvents BrF_3 and HSO_3F has been described elsewhere.⁴

Sample Preparation. All manipulations of volatile materials were carried out under anhydrous conditions on a vacuum line constructed from 316 stainless steel, nickel, Teflon, and FEP. Solid materials were transferred in a nitrogen-filled drybox.

NMR samples were prepared in preweighed sample tubes (5-mm o.d. for ^{19}F and 10-mm o.d. for ^{129}Xe) attached to Teflon or FEP valves

(15) S. M. Williamson, *Inorg. Synth.*, **11**, 67 (1968).

(16) C. L. Schack and R. D. Wilson, *Inorg. Chem.*, **9**, 311 (1970).

(17) J. H. Holloway and G. J. Schrobilgen, submitted for publication in *Inorg. Chem.*

(14) R. J. Gillespie and G. J. Schrobilgen, *Inorg. Chem.*, **13**, 1694 (1974).

by means of $1/4$ -in. Teflon nuts and compression fittings. In the case of samples containing BrF_3 or SO_2ClF solvent, the solvent was condensed onto an appropriate quantity of solute(s) at -196°C . Fluorosulfuric acid samples were prepared in a drybox by syringing the solvent into a sample tube containing the solute(s) cooled to -196°C . Samples were warmed briefly to -48°C to effect dissolution. All samples were stored at -196°C until their spectra could be recorded.

NMR Instrumentation and Spectra. ^{19}F NMR spectra were recorded in CW mode on a JEOL PS-100 NMR spectrometer operating at 94.1 MHz and equipped with a low-temperature controller. All spectra were recorded in field-sweep mode and externally locked to D_2O . The pulse FT ^{129}Xe NMR instrumentation has been described elsewhere.⁹

The chemical shift convention is that outlined by IUPAC;¹⁸ i.e., a positive chemical shift denotes a positive frequency and vice versa with respect to the designated reference substance. All spectra were

referenced externally: ^{19}F , neat CFCl_3 at the quoted sample temperature; ^{129}Xe , neat XeOF_4 at 25°C .

Acknowledgments. We thank the National Research Council of Canada for the award of an Overseas Postdoctoral Fellowship (G.J.S.) and the Science Research Council of Great Britain for operational grant support. We are particularly indebted to Professor Pierre Granger (IUT de Rouen, Rouen, France) for his assistance in obtaining the ^{129}Xe NMR spectra and to Professors R. J. Gillespie (McMaster University, Hamilton, Canada) and M. C. R. Symons (Leicester University, Leicester, England) for reading the paper and offering useful suggestions for its improvement.

Registry No. WOF_4 , 13520-79-1; MOF_4 , 14459-59-7; $\text{XeF}_2\cdot 2\text{WOF}_4$, 56174-65-3; $\text{XeF}_2\cdot 2\text{MoOF}_4$, 65651-37-8; $\text{XeF}_2\cdot \text{WOF}_4$, 55888-48-7; $\text{XeF}_2\cdot \text{MoOF}_4$, 74080-83-4; XeF_2 , 13709-36-9; $\text{XeF}_2\cdot \text{MoOF}_4(\text{MoOF}_4)_2$, 65622-63-1; $\text{XeF}_2\cdot \text{MoOF}_4(\text{MoOF}_4)_3$, 74037-08-4; $\text{XeF}_2\cdot \text{WOF}_4(\text{WOF}_4)_2$, 65622-72-2; $\text{FXeO}\cdot \text{WF}_3(\text{WOF}_4)$, 74037-07-3; $\text{FXeO}\cdot \text{WF}_3(\text{WOF}_4)_2$, 74050-90-1; $\text{FXeO}(\text{F})\text{S}(=\text{O})\text{OMoOF}_4$, 74080-82-3; FXeOSO_2F , 25519-01-1.

(18) "Recommendations for the Presentation of NMR Data for Publication in Chemical Journals", *Pure Appl. Chem.*, **29**, 627 (1972); **45**, 217 (1976).

Contribution from the Department of Chemistry,
University of California, Santa Barbara, California 93106

Photochemistry of Diacidobis(ethylenediamine)iridium(III) Complexes, *cis*- and *trans*- $\text{Ir}(\text{en})_2\text{XY}^{n+}$. Observations Regarding the Photoisomerization of d^6 Complexes

MEHDI TALEBINASAB-SARVARI¹ and PETER C. FORD*

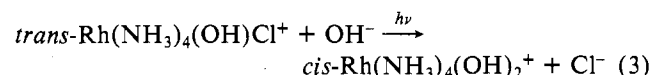
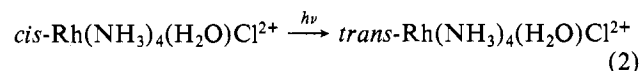
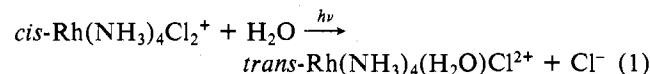
Received January 30, 1980

Ligand field excitation of the bis(ethylenediamine)iridium(III) complexes *cis*- and *trans*- $\text{Ir}(\text{en})_2\text{XY}^+$ ($\text{X} = \text{Y} = \text{Cl}^-$, Br^- , or I^- ; $\text{X} = \text{OH}^-$, $\text{Y} = \text{Cl}^-$) in aqueous solution leads to halide photolabilization in each case. For the *cis*- and *trans*-dichloro complexes, quantum yields were independent of solution pH, displaying the same values in acidic and basic solutions. In acidic solution, the *trans*-dihalo complexes undergo photoaquation to give *trans*- $\text{Ir}(\text{en})_2(\text{H}_2\text{O})\text{X}^{2+}$ with complete retention of configuration. However, the *cis* analogues undergo some concomitant photoisomerization to give a mixture of *trans*- and *cis*- $\text{Ir}(\text{en})_2(\text{H}_2\text{O})\text{X}^{2+}$ with the extent of photoisomerization following the order $\text{Cl}^- < \text{Br}^- < \text{I}^-$. In acidic solution, *trans*- $\text{Ir}(\text{en})_2(\text{H}_2\text{O})\text{Cl}^{2+}$ is apparently photoinert (H_2O exchange excluded) while the *cis* analogue undergoes photoisomerization to the *trans* isomer with a modest quantum yield (0.03 mol/einstein). Making solutions of these ions alkaline (pH 12) gives the hydroxo analogues which demonstrate dramatically different photoreaction behavior, *cis*- $\text{Ir}(\text{en})_2(\text{OH})\text{Cl}^+$ undergoing Cl^- labilization to give *cis*- $\text{Ir}(\text{en})_2(\text{OH})_2^+$ and *trans*- $\text{Ir}(\text{en})_2(\text{OH})\text{Cl}^+$ undergoing concomitant photohydrolysis/photoisomerization to give the same product. These results are interpreted in terms of the model proposed earlier to explain the photostereochemistry of similar rhodium(III) complexes.

Introduction

The stereochemical properties of d^6 hexacoordinate complexes as the result of ligand field (LF) excitation have been the subject of much recent interest.²⁻⁸ The photostereo-

chemistry of rhodium(III) amine complexes has proved especially rich with recent results stimulating several related models^{2a,6,7} to rationalize these. A series of observations made in these laboratories with the rhodium(III) tetraammines illustrate the types of photoreactions seen in these systems (eq 1-3). Both *cis* and *trans* to *cis* isomerization of the



$\text{Rh}(\text{III})$ tetraammines can be effected by LF excitation, depending upon the balance of the ligand field. In addition for

- (1) (a) Taken in part from the Ph.D. dissertation of M.T.-S., University of California, Santa Barbara, 1979. (b) Reported in part at the 177th National Meeting of the American Chemical Society, Honolulu, Hawaii, April 1979.
- (2) (a) Strauss, D.; Ford, P. C. *J. Chem. Soc., Chem. Commun.* **1977**, 194. (b) Skibsted, L.; Strauss, D.; Ford, P. C. *Inorg. Chem.* **1979**, *18*, 3171. (c) Skibsted, L.; Ford, P. C. *J. Chem. Soc., Chem. Commun.* **1979**, 853. (d) Skibsted, L.; Ford, P. C. *Inorg. Chem.* **1980**, *19*, 1828.
- (3) (a) Petersen, L. D.; Jakse, F. P. *Inorg. Chem.* **1979**, *18*, 1818. (b) Clark, S. F.; Petersen, J. D. *Ibid.* **1979**, *18*, 3394.
- (4) (a) Martins, E.; Sheridan, P. S. *Inorg. Chem.* **1978**, *17*, 2822. (b) *Ibid.* **1978**, *17*, 3631. (c) Sheridan, P. S.; Adamson, A. W. *J. Am. Chem. Soc.* **1974**, *96*, 3032.
- (5) Muir, M.; Huang, W. L. *Inorg. Chem.* **1973**, *12*, 1831.
- (6) Vanquickenborne, L. G.; Ceulemans, A. *Inorg. Chem.* **1978**, *17*, 2730.
- (7) Petersen, J. D.; Purcell, K., submitted for publication. Private communication from Dr. Petersen, reported in part at the 174th National Meeting of the American Chemical Society, Chicago, Ill., Sept 1977.

(8) Sellan, J.; Rumfeldt, R. *Can. J. Chem.* **1976**, *54*, 519, 1061.